An Overview of Computational Fluid Dynamics as a Tool to Support Ultrasonic Flow Measurements

Article *in* Metrology · February 2025

DOI: 10.3390/metrology5010011

4 authors:

Guilherme Siqueira de Aquino
Institute of Fluid Mechanics of Toulouse, French National Centre for Scientific Research
5 PUBLICATIONS **16** CITATIONS
SEE PROFILE

Ramon Silva Martins
Federal University of Espírito Santo
59 PUBLICATIONS **163** CITATIONS
SEE PROFILE

Marcio Ferreira Martins
Federal University of Espírito Santo
109 PUBLICATIONS **909** CITATIONS
SEE PROFILE

Rogerio Ramos
Federal University of Espírito Santo
77 PUBLICATIONS **215** CITATIONS
SEE PROFILE

metrology

MDPI

Review

An Overview of Computational Fluid Dynamics as a Tool to Support Ultrasonic Flow Measurements

Guilherme Siqueira de Aquino [1,2,†], Ramon Silva Martins [1,2,*], Marcio Ferreira Martins [2] and Rogério Ramos [1]

[1] Research Group for Oil and Gas Flow and Measurement (NEMOG), Federal University of Espírito Santo, Av. Fernando Ferrari, 514, Vitória 29075-910, ES, Brazil; guilherme.siqueiradeaquino@imft.fr (G.S.d.A.); rogerio.ramos@ufes.br (R.R.)

[2] Multiphysics Modeling Laboratories (MMLabs), Federal University of Espírito Santo, Av. Fernando Ferrari, 514, Vitória 29075-910, ES, Brazil; marcio.martins@ufes.br

* Correspondence: ramon.martins@ufes.br

† Current address: Institut de Mécanique des Fluides de Toulouse (IMFT), Université de Toulouse, CNRS, 31400 Toulouse, France.

Abstract: Ultrasonic flow meters (UFMs) by transit time are ubiquitous in industrial applications, mainly for their versatility and practicality. They are widely used in gas and liquid installations, such as the oil and gas industry or feedwater systems in nuclear power plants. Computational fluid dynamics (CFD) techniques can be used as a tool to potentially improve the ultrasonic flow measurements. CFD may contribute to predicting the velocity profile and the profile factor in disturbed flows, integrating fluid flow and acoustic ray, improving the calibration of UFMs, or assisting in design optimization. This communication presents the working principle of the UFM, discusses how CFD can be used as a tool to support improvements, and shows relevant trending fields that deserve further investigation to promote significance on this subject.

Keywords: ultrasonic flow meter; clamp on; transit time; CFD; flow meter; profile factor

Academic Editor: Han Haitjema

Received: 26 November 2024
Revised: 20 December 2024
Accepted: 27 January 2025
Published: 5 February 2025

Citation: Siqueira de Aquino, G.; Silva Martins, R.; Ferreira Martins, M.; Ramos, R. An Overview of Computational Fluid Dynamics as a Tool to Support Ultrasonic Flow Measurements. *Metrology* **2025**, *5*, 11. https://doi.org/10.3390/metrology5010011

1. Introduction

Ultrasonic flow meters (UFMs) are used in a wide range of industrial applications to measure the flow rate of fluids flowing through pipes. Flow rate measurement is essential in any industrial process involving pipe flow, ranging from ordinary operational measurement and custody transfer, which serves as a cash register for accounting for production, to environmental control and monitoring, such as in the measurement of greenhouse gas emissions in oil rigs. Among various other consolidated technologies, the transit time ultrasonic flow measurement presents a solution to several challenges in different applications due to its inherent characteristics, such as high operation range, good accuracy, low maintenance costs, high turn-down ratio, and the possibility of self-diagnosis [1,2]. Furthermore, the UFM also operates with variations in fluid chemical compositions and supports the presence of impurities in the flow [3]. The characteristics mentioned above make the UFM a high commercial success when using this meter to measure the flow rate of liquids or gases, both flammable and non-flammable, in low or high pressure or temperature. It is worth noting that transit time is not the only ultrasonic measuring principle possible. Ultrasonic flow measurements can also be made by the Doppler effect, mainly used in two-phase flows [4], but this is outside the scope of the present communication.

Among the various potential applications of the ultrasonic flow meter, some stand out for their environmental significance in the current global context. One of them is the use of UFMs in flare gas systems. Basically, the gas flaring process is used as a safety procedure to relieve over-pressure events that may occur throughout production on onshore and offshore oil and gas rigs, responsible for the emission of 350 million tons of carbon dioxide equivalent each year in the world [5]. It involves the burning of natural gas (mainly methane [6]), a by-product of crude oil extraction, leading to the emission of air pollutant compounds—at least, nitrogen oxides (NO_x), sulfur oxides (SO_x), carbon dioxide (CO_2), hydrogen sulfide (H_2S), and particulate matter (PM) [7]. Motivated to reduce the environmental impacts of habitual flaring gas and its economic losses due to the high heating value [6,8], both public policies and developing/improving technologies are essential. Further, policy efforts continue to develop strategies to reduce flaring [9–11]. In this way, the UFM plays an essential role in estimating the greenhouse gas emission in flare gas processes, once the flow rate can be used to assess it [2,12]. Another equally important application of UFMs is in water supply chains. On this, the UFM could be used to identify leaks and help understand consumption patterns, reducing water waste [13]. Furthermore, the UFM is also used in applications in aerospace exploration [14], in nuclear power plants [15], and in feed water systems [16], making it ubiquitous in industrial pipe flow rate measurements.

In the scenario where the correct measurement is essential from both the economic and environmental points of view, the necessity of low measurement uncertainty becomes stricter (e.g., in the flare gas context, a typical maximum uncertainty is 5% [17]). Unlike certain flow measurement technologies (such as Coriolis or electromagnetic flow meters), the accuracy of the UFM is highly dependent on the prior knowledge of the flow velocity profile in the pipe stretch where the UFM is installed. In this way, those meters are typically designed to work under turbulent, fully developed flows (i.e., unidimensional symmetric mean velocity profile condition at the installation section). Meanwhile, dealing with non-conforming conditions in ultrasonic flow measurement installations is expected due to the presence of valves, curves, diameter changes, and other devices or piping changes, leading to an asymmetric velocity profile. Therefore, a significant error source is associated with the velocity profile [18]. Any deviation from the ideal fully developed condition requires the UFM control system's reconfiguration to maintain the required levels of uncertainty. This leads to some options to attenuate or evaluate the effect of profile asymmetries on the UFM: (i) install the UFM on a straight section long enough so that a fully developed condition is reached, (ii) measure the velocity profile downstream from the meter by velocity anemometers (hot wire, laser Doppler or particle image velocimetry), (iii) install the UFM with multiple acoustic channels to compensate the effect of velocity profile asymmetries, or (iv) perform numerical simulations using computational fluid dynamics (CFD) on a given pipeline configuration to obtain the velocity profile at the measuring section or to infer the optimum installation configuration. When the measuring section is placed far enough from the aforementioned sources of flow disturbance, the mean flow reaches the so-called fully developed condition, allowing the meter to be calibrated for a fully developed velocity profile. However, this scenario is mainly impractical in the industry due to the pipe length requirement to reach these conditions (usually longer than 20 pipe diameters) [19]. Experimental techniques to obtain the velocity profile remain limited to laboratory analysis [20]. In addition, the use of multi-path flow measurement could increase the cost of the measurement, making it unfeasible in various conditions due to economic reasons. The remarkable advancements of numerical methods in CFD, processing capability, and the eventual popularization of the use of commercial codes in industrial applications makes CFD an essential tool for contributing to ultrasonic flow measurement (for examples of successful application of CFD for these purposes, see Refs. [19,21–26]).

Ultrasonic flow measurement is actually a multiphysics problem since it involves at least fluid dynamics, thermodynamics, acoustics, and signal processing. Dealing with this multiphysics characteristic is not trivial, and assumptions are often used to simplify some of the physics and focus on the desired one(s). In this context, the main contribution of CFD is on fluid dynamics, solving the Navier–Stokes equations to obtain the pressure and velocity field in the domain of interest (i.e., the digital replica after a series of simplifications of the plant where the UFM is/will be installed). Thereafter, CFD could support the analysis to reduce the flow measurement uncertainty [19,25]. Typically, UFM works in turbulent flow conditions. To represent turbulence, it is possible to either resolve all scales of motion through direct numerical simulation (DNS) or employ modeling approaches. Two common methods include the Reynolds-Averaged Navier–Stokes (RANS) approach, which models the effects of all fluctuating turbulent quantities, and Large Eddy Simulations (LES), which focuses on solving the larger and more energetic eddies while modeling the smaller, more dissipative time scales. In this scenario, the huge computation effort in simulating complex geometries and high Reynolds numbers using LES and DNS approaches makes it impractical. Thus, RANS is often preferred for industrial applications, compromising the accuracy, as it is not the most accurate to simulate flows in complex geometries [27]. The use of CFD with the RANS approach presents the existence of many modeling parameters, such as interpolation schemes, turbulence models, and the influence of spatial discretization. The influence of those parameters has been evaluated in previous works [19,25]. Nonetheless, it is essential to systematically obtain coherent results in CFD simulations for UFMs to achieve metrological representativeness.

Aiming to cover the recent remarkable technological advances in the use of CFD for supporting ultrasonic flow measurements, this text provides a comprehensive review of the application of CFD for this purpose from the viewpoint of fluid mechanics. The text focuses on transit time ultrasonic flow measurements for single-phase flow applications considering the acoustic path as a straight line. It is assumed that the device works properly and the acoustic path is well established; thus, signal attenuation, flow composition, or signal treatments are not assessed here. The paper is organized as follows: the physical principle of ultrasonic flow measurement is presented in Section 2, providing the UFM working principle. Additionally, in Section 2, different installation configurations are shown aiming to represent typical industrial applications. An overview of how CFD has been used to improve the UFM measurements is presented in Section 3. Section 4 resumes the perspectives for future investigations and technologies via CFD to improve the performance of UFMs. Further remarks are presented in Section 5.

2. Physical Principle of Ultrasonic Flow Measurement and Installations Configurations

Due to the versatility of ultrasonic flow measurement technology, various configurations are available depending on the specific application. The fundamental working principle remains consistent: at least two piezoelectric transducers are positioned at a predetermined distance, angle, and arrangement. These transducers convert electrical signals into ultrasonic waves and vice versa. Consequently, the transducers work as both transmitters and receivers alternately. The emitted mechanical wave departs from the transducer acting as a transmitter, travels through the fluid, and reaches the transducer acting as a receiver after a specific travel time. Effectively, the UFM measures the time the wave travels from one transducer to the other. This time interval between the emission and reception of the ultrasonic pulse is called the *time-of-flight* and is proportional to the fluid velocity [28]. The transducers are made of a piezoelectric material that is excited in a high frequency ranging from 20 kHz to several MHz, varying depending on the application

(e.g., in the order of kHz for gas measurements [29] and MHz for liquid [30]). Indeed, the resultant mechanical wave is an ultrasonic wave (i.e., the frequency is more significant than 20 kHz—above the audible range for humans). When emitted, the wave propagates through space, creating a wavefront that spreads outward. Due to geometrical conditions, these wavefronts concentrate more energy along a preferential path, called the *acoustic path*. Depending on the medium, ultrasonic waves travel at a given velocity c_i. In fluids, this velocity depends, at least, on the thermodynamic state of the fluid, like density ρ_f, temperature T_f, and chemical composition [18]. While in solids (here, the interest is in the pipe wall and in the transducer itself), it depends on the material density ρ_m, but also on the material treatment during the manufacture [31]. As a result, the time it takes for the wave to reach the other transducer varies when it interacts with the pipe wall. Depending on the UFM technologies, a transducer can be installed inside or outside the pipe. The transducers are placed inside the pipeline in the *wetted transducer* configuration. In contrast, in the *clamp-on* configuration, the transducers are positioned outside the pipeline in a non-intrusive manner. For the purposes of this discussion, the speed of sound in the fluid and the pipe wall will be denoted as c_f and c_w, respectively. Additionally, the speed of sound in the transducer material will be represented as c_{UFM}.

Here, the text is limited to time-of-flight ultrasonic flow meters in two configurations: (i) wetted transducers and (ii) clamp-on. Those meters can be used in single- or multi-path approaches, leading to different possibilities in the transducers' arrangement. Therefore, an overview of multi-path applications and their effects is also presented.

2.1. Wetted Transducers

In Figure 1, the overview of the physical principle for a single-path wetted transducer UFM is shown. A schema of the UFM installation is presented in Figure 1a. First, the plane Ω is defined; this plane represents the plane where the transducers interact, also called the *emission plane*. The plane orientation is given by the angle θ—the angle between the plane and the y-coordinate. The other Cartesian coordinates x and z are defined following the right-hand rule. Figure 1b presents the transducers for a single-path configuration. The transducers are installed through a cavity, and their tip usually faces the internal pipe wall (see Figure 1c), meaning the sound wave only interacts with the fluid. The flow streamwise direction is aligned with the x coordinate. An exaggerated example of the acoustic path trajectory is presented with length L_{AP} for visualization purposes. Note that the acoustic path deviates from a straight line due to the interaction with the fluid flow. Nonetheless, for flow velocities much smaller than the velocity of the sound in the fluid (i.e., $U/c_f < 0.1$, with U being the fluid velocity), it is reasonable to approach this curve as a straight line [32]. In the following, the acoustic path is considered as a straight line.

The main dimensions and variables are presented in Figure 1c. The pipe inner diameter is D, and the distance between the transducers is L. The transducers are installed with an angle α related to the $-x$ coordinate. As mentioned, both the transducers act as transmitters and receivers. Nonetheless, one transducer (transducer **a** in Figure 1) sends the ultrasound pulse upstream, while the other one (transducer **b** in Figure 1) goes downstream. In the absence of the fluid flow, the time-of-flight is the same for both cases independently, in which each of the transducers acts as receiver or transmitter: $t = c_f/L_{\text{AP}}$. In the flow presence, the flow influences the ultrasound pulse, making the time-of-flight dependent on each transducer acting as the emitter or receiver. When transducer **a** acts as the emitter and **b** acts as the receiver, the time-of-flight is given by t_{ab}, and in the next cycle, transducer **b** acts as the emitter and **a**, as the receiver, yielding t_{ba}. It is important to note that $t_{\text{ba}} > t_{\text{ab}}$. This is because the pulse emitted by the upstream transducer is accelerated by the flow, which decreases the time needed for it to reach the other transducer. Conversely, the pulse

emitted by the downstream transducer travels in the opposite direction against the flow, which causes it to take longer to reach the upstream transducer. These times are related to the projection of the fluid mean velocity along the acoustic path $\overline{U}_{\mathrm{AP}}$ by the given equations:

$$t_{\mathrm{ab}} = \frac{L_{\mathrm{AP}}}{c_f + \overline{U}_{\mathrm{AP}}} + t_0 \,, \tag{1}$$

$$t_{\mathrm{ba}} = \frac{L_{\mathrm{AP}}}{c_f - \overline{U}_{\mathrm{AP}}} + t_0 \,. \tag{2}$$

Here, t_0 is the time taken from the ultrasonic pulse travel through the transducer proportional to the transducer's constructive material characteristics. As $t_0 << t_{\mathrm{ab}}$, this time it is not considered here.

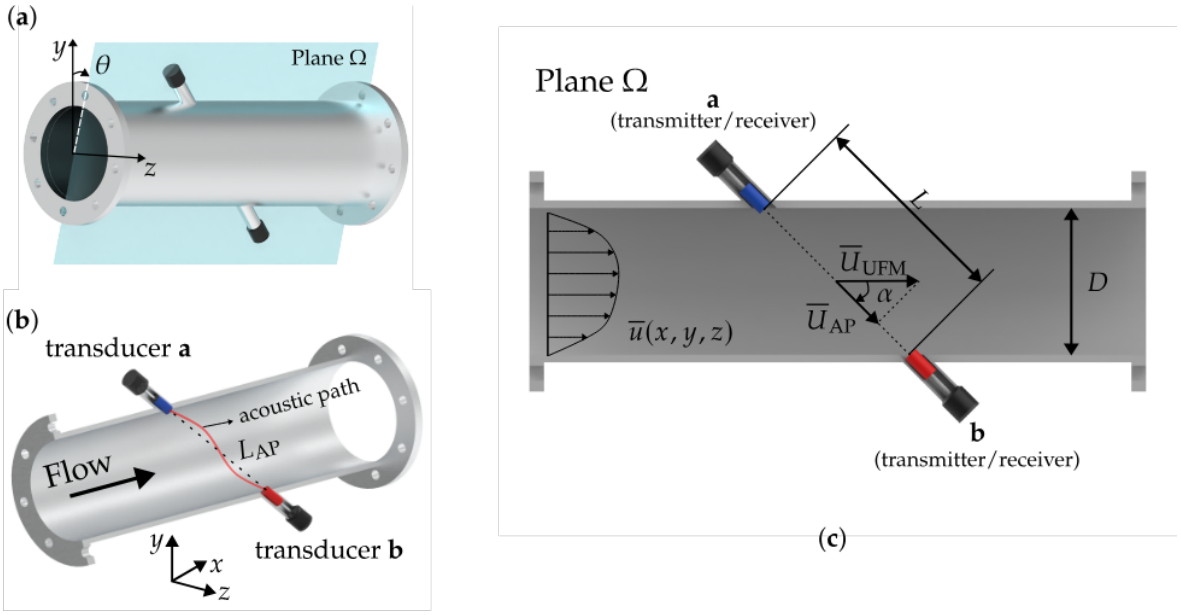

Figure 1. Schematic of a single-path wetted transit-time ultrasonic flow meter. (**a**) A schema of a possible installation configuration, in which θ represents the angle between the Cartesian coordinates y and z. (**b**) The two transducers (**a** and **b**) are present, acting both as transmitters and receivers. The wave trajectory length is given by L_{AP} following the acoustic path. The fluid flows along the x-direction (streamwise direction). (**c**) The main variables and dimensions are shown. D is the inner pipe diameter, and L is the length separating the transducers installed at a given angle α related to the streamwise direction. U_{AP} is the projected mean velocity along the acoustic path, while U_{UFM} is the mean streamwise flow velocity along the acoustic path.

The streamwise velocity along the acoustic path is $\overline{U}_{\mathrm{UFM}}$, which is related to $\overline{U}_{\mathrm{AP}}$ by the geometrical relation:

$$\overline{U}_{\mathrm{UFM}} = \frac{\overline{U}_{\mathrm{AP}}}{\cos\alpha} \,, \tag{3}$$

and, by definition, $\overline{U}_{\mathrm{AP}}$ is,

$$\overline{U}_{\mathrm{AP}} = \frac{1}{L_{\mathrm{AP}}} \int_{L_{\mathrm{AP}}} \vec{u}(x,y,z) \cdot d\vec{L} \,, \tag{4}$$

in which $\vec{u}(x, y, z)$ is the velocity field with three-dimensional velocity components u, v, and w in the x, y, and z direction, respectively. To associate the time-of-flight measured by the transducers and $\overline{U}_{\mathrm{UFM}}$, Equations (1) and (2) are solved to obtain the following relation:

$$\overline{U}_{\mathrm{UFM}} = \frac{D}{\sin 2\alpha}\left(\frac{t_{\mathrm{ba}} - t_{\mathrm{ab}}}{t_{\mathrm{ab}} t_{\mathrm{ba}}}\right). \tag{5}$$

From the resolution of the same system of equations, the velocity of the sound is also obtained, given by,

$$c = \frac{D}{2\sin\alpha}\left(\frac{t_{\mathrm{ba}} + t_{\mathrm{ab}}}{t_{\mathrm{ab}} t_{\mathrm{ba}}}\right); \tag{6}$$

this indicates that UFM also measures the velocity of the sound through the fluid.

When the meter is installed under high flow velocity conditions ($\overline{U}_{\mathrm{UFM}} \gtrsim 80$ m/s) in large diameter pipelines ($D > 2$ in), the ultrasonic beam can be highly affected by the flow suffering a large drift, increasing the measurement error. Therefore, one possible technological solution is to use an intrusive configuration where the transducers are positioned on the same side of the pipe, creating a path that is parallel to the flow, as shown in Figure 2, that can be installed either in the vertical or horizontal positions. As the path is shorter, it is less susceptible to this drift. Additionally, the transducers' positioning reduces the potential for signal loss, ensuring consistent data collection across a broad range of flow rates [3]. Otherwise, the UFM probes need to be at a specific vertical (or horizontal) positions (h_v in Figure 2), and any deviation (e.g., due to the asymmetry in the flow field) could lead to inaccurate measurements. As this solution is under development, there is a lack of scientific studies to understand how sensitive it is to variations from the idealized condition. Further investigation into this topic should be interesting for the current technological development.

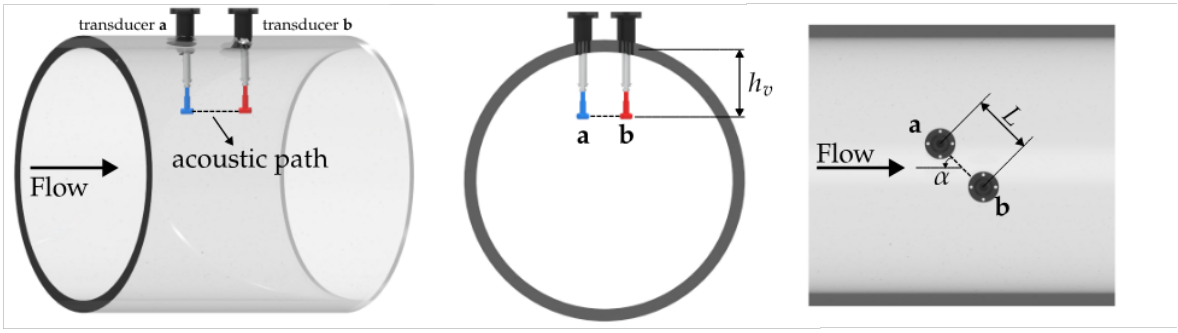

Figure 2. Intrusive installation of wetted ultrasonic flow meter. The following main dimensions are presented: h_v the vertical installation position, L the distance between transducers **a** and **b**, and α the angle between the acoustic path and streamwise direction.

2.2. Clamp-On

Another widely-used UFM variation is the clamp-on arrangement. Unlike the wetted transducer configuration, the sensors are attached externally to the pipe wall. Note that the installation does not require any interruption or modification to the pipe, making it a non-intrusive, non-obstructive, and easy-to-install configuration [33].

There are several ways to arrange the transducers, which can lead to different configurations. Some examples of market-available configurations are represented in Figure 3. In Figure 3a–c, V-shaped, W-shaped, and Z-shaped UFMs are shown.

Besides the configuration used, the working principle remains the same: effectively, the UFM measures the time-of-flight between at least two transducers. Therefore, the procedure is nearly the same as that presented in Section 2.1. The relation between the

mean streamwise flow velocity U_{UFM} and the measured time-of-flight are derived from the geometrical and physical relations inherent to the configuration. To represent this procedure, a V-shaped type configuration is chosen. An overview of this mounting is shown in Figure 4.

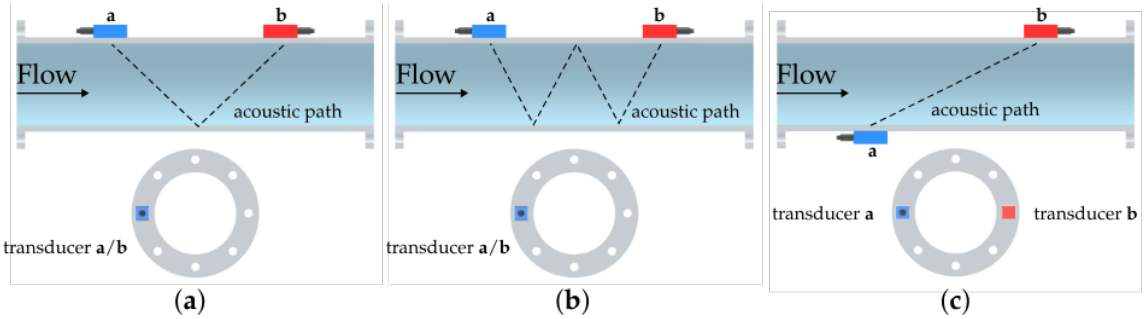

Figure 3. Representation of different installation configurations for clamp-on ultrasonic flow meters. (**a**) Type V-shaped. (**b**) Type W-shaped. (**c**) Type Z-shaped.

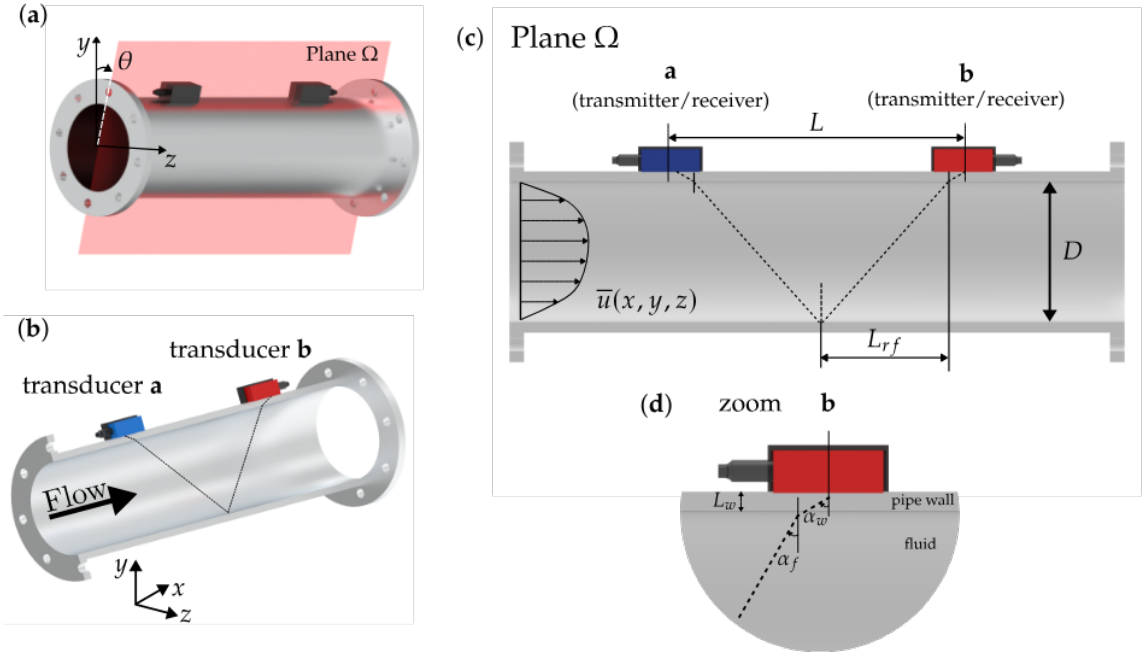

Figure 4. Schematic of a clamp-on ultrasonic flow meter installed in a V-shaped configuration. (**a**) A three-dimensional visualization of a possible installation configuration, in that θ represents the angle between the Cartesian coordinates y. (**b**) Transducers **a** and **b** are presented; both act as transmitters and receivers. The fluid flows along the x direction (streamwise direction). (**c**) The main dimensions are shown. D is the inner pipe diameter, L is the length separating the transducers, and L_{rf} is the distance between the position where the ultrasonic beam begins to propagate in the fluid and the point where the ultrasonic wave reflects on the wall. (**d**) Details in the region of transducer **b**: angles α_w and α_f are the refraction angles of the pipe wall (with thickness L_w) and fluid, respectively.

The three-dimensional installation visualization is presented in Figure 4, with the plane Ω given as the plane where the transducers interact, oriented by the angle θ, as in the wetted configuration. The process of sending and receiving the ultrasonic pulse differs from the procedure in Section 2.1. The transducers are installed outside the pipe, and the acoustic path has the length L_{AP} reflecting at the pipe wall (See Figure 4b). Thus, the wave travels through the pipe wall before traveling to the fluid. The ultrasonic wave travels in different materials at different speeds depending on the material's properties. Therefore, the sound

wave suffers refraction when crossing the material boundaries (from the pipe wall to the fluid and from the fluid to the pipe wall). These phenomena are highlighted in Figure 4c, where the pipe wall thickness is L_w and the refraction angle is α_w. The distance between the position where the ultrasonic beam begins to propagate in the fluid and the point where the ultrasonic wave reflects is L_{rf} and the fluid refraction angle is α_f. The refraction is governed by Snell's law, expressed as:

$$\frac{\sin \alpha_w}{c_w} = \frac{\sin \alpha_f}{c_f} = \frac{\sin \alpha_{\text{UFM}}}{c_{\text{UFM}}}\,, \tag{7}$$

where α_{UFM} and c_{UFM} are the refraction angle and the speed of the sound in the ultrasonic flow meter, respectively.

Different from the principle shown in Section 2.1, the ultrasonic beam also travels in the pipe wall. The transit time that the beam takes when not in the liquid (transducer and wall) is hereafter called t_{delay}, being:

$$t_{\text{delay}} = 2\left(\frac{L_w / \cos \alpha_w}{c_w} + t_0\right). \tag{8}$$

For the clamp-on, the value of t_0 could be in the order of magnitude of the time it takes for the ultrasonic pulses to travel through the wall. Thus, it is considered in the time calculation. Using the geometric relations presented in Figure 4c, it is possible to obtain the time necessary for the ultrasound beam to travel through the fluid until it reaches the other transducer, following the trigonometry relations $L_{\text{AP}} = D/\cos \alpha_f$ and $\overline{U}_{\text{AP}} = \overline{U}_{\text{UFM}} \sin \alpha_f$:

$$t_{\text{ab, fluid}} = \frac{2D}{\cos \alpha_f (c_f + \overline{U}_{\text{UFM}} \sin \alpha_f)}\,, \tag{9}$$

$$t_{\text{ba, fluid}} = \frac{2D}{\cos \alpha_f (c_f - \overline{U}_{\text{UFM}} \sin \alpha_f)}\,. \tag{10}$$

Resolving for $\overline{U}_{\text{UFM}}$:

$$\overline{U}_{\text{UFM}} = \frac{t_{\text{ba,fluid}} - t_{\text{ab,fluid}}}{t_{\text{ba,fluid}} + t_{\text{ab,fluid}}}\left(\frac{c_f}{\sin \alpha_f}\right). \tag{11}$$

Nonetheless, the time needed for the ultrasonic wave to travel through the whole system (transducer, wall, and fluid) has to consider the delay time:

$$t_{\text{ab}} = t_{\text{ab,fluid}} + t_{\text{delay}}\,, \tag{12}$$

$$t_{\text{ba}} = t_{\text{ba,fluid}} + t_{\text{delay}}\,, \tag{13}$$

thus,

$$\overline{U}_{\text{UFM}} = \frac{t_{\text{ba}} - t_{\text{ab}}}{t_{\text{ba}} + t_{\text{ab}} - 2t_{\text{delay}}}\left(\frac{c_f}{\sin \alpha_f}\right). \tag{14}$$

Finally, applying Snell's law:

$$\overline{U}_{\text{UFM}} = \frac{t_{\text{ba}} - t_{\text{ab}}}{t_{\text{ba}} + t_{\text{ab}} - 2t_{\text{delay}}}\left(\frac{c_{\text{UFM}}}{\sin \alpha_{\text{UFM}}}\right). \tag{15}$$

2.3. Multi-Path

Another strategy is to use multiple pairs of transducers to obtain various measurements, which increases measurement accuracy. This approach can be used in both configurations mentioned above. The procedure calculates the average value of the flow mean

streamwise velocity measured by the different pairs of sensors; the expression is presented in Equation (16).

$$\langle \overline{U}_{\mathrm{UFM}} \rangle = \frac{1}{n} \sum_{i=1}^{n} \omega_i \overline{U}_{\mathrm{UFM},i} \, , \tag{16}$$

where n is the number of acoustic paths, i represents the the i-th acoustic path, and $\overline{U}_{\mathrm{UFM},i}$ is the velocity measurement associate with it. Additionally, the factor ω_i gives the contribution of the i-th, which is determined in the integration algorithm [34]. In this way, various combinations of arrangements between the pair of transducers can be used. To illustrate the multi-path UFM, some examples of possible mounting possibilities are presented in Figure 5 for both wetted transducer and clamp-on configurations. For the wetted transducer, the configuration is the six paths used in the measurement of hot pulsating gases [35], while for the clamp-on, the multi-path using two paths in a Z shape is presented.

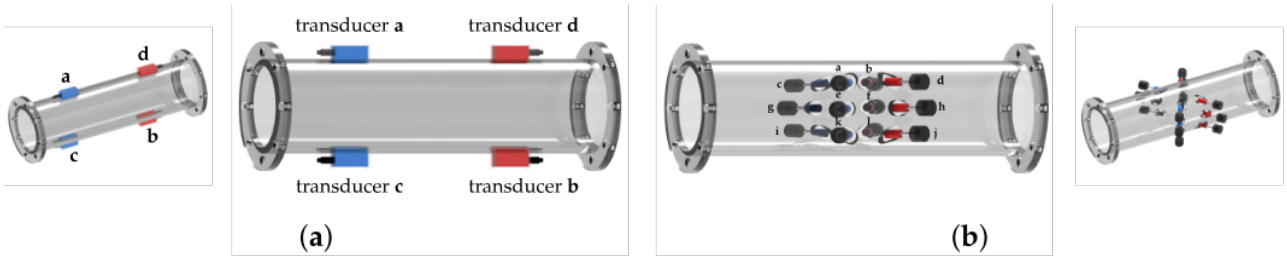

Figure 5. Illustration of possible multi-path installations. (**a**) Clamp-on multi-path in Z shape; two acoustic paths are created by the pairs of transducers (**a** and **b**) and (**c** and **d**). (**b**) Wetted transducers 6-paths configuration; the transducer indices are presented by (**a**–**j**).

Different strategies can be processed by setting up multiple paths, such as in phase array technology. Unlike traditional ultrasonic transducers, phased array transducers sweep ultrasonic beams electronically, reducing the number of transducers needed while maintaining precision. By applying a flexible, generalized velocity model that integrates symmetric and asymmetric flow profiles and using Gaussian quadrature integration, the flowmeter achieves high accuracy in diverse flow conditions, including complex disturbed flows [36]. Another strategy is using an averaging method for reference waves across multiple acoustic paths. Rather than relying on a single reference signal, the system averages multiple upstream and downstream waveforms, which reduces the impact of noise and waveform distortion that can arise from high gas velocities and other factors, like piping arrangement disturbances. By assigning each path its own reference wave, the system achieves more precise time-of-flight detection and calculations for each acoustic path, leading to a more accurate processing and measurement of cross-sectional gas flow velocity. This approach offers significant advantages, including improved accuracy, noise resilience, and consistency in flow rate measurements, making it particularly effective for applications requiring precise gas flow monitoring in large pipelines [34]. Otherwise, besides great advances in the multi-path techniques, the increase in the financial cost associated with the measurements makes it impractical for various applications, making the single-path flow meter the most used and preferable for many applications (such as in flare gas measurements and water waste monitoring [13,25]).

2.4. Converting the Measured Time-of-Transit into the Flow Rate: Profile Factor

The UFM measurement gives the streamwise velocity U_{UFM} along the acoustic path. Then, the procedure is to associate this velocity with the flow rate. For that, the so-called

profile factor (or simple k factor), a ratio between the mean velocity in the cross-section and the mean streamwise velocity along the acoustic path, is defined [28,37]:

$$k = \frac{\overline{U}_m}{\overline{U}_{\mathrm{UFM}}} = \frac{\frac{1}{A}\int_A \vec{u}(x,y,z)\cdot d\vec{A}}{\frac{1}{\cos\alpha}\frac{1}{L_{\mathrm{AP}}}\int_{L_{\mathrm{AP}}} \vec{u}(x,y,z)\cdot d\vec{L}}\,, \tag{17}$$

where A is the area of the pipe cross-section and $d\vec{A}$ is the differential area element. Finally, the flow rate Q can be calculated as follows [19],

$$Q = k\overline{U}_{\mathrm{UFM}}A\,. \tag{18}$$

It is worth noting that the flow rate is directly proportional to the profile factor. This factor must be implemented a priori on the flow rate computer. Any deviation between the implemented value and the real flow conditions leads to inaccurate flow rate measurements.

As seen explicitly in Equation (17), prior knowledge of the velocity field along the acoustic path is necessary to calculate the flow rate. In this manner, it is necessary to define strategies to obtain the velocity distribution along the acoustic path. This section presents the usual approaches for the two possible scenarios: fully developed and disturbed flows.

For a fully developed turbulent flow, the velocity field reduces to the time-averaged velocity $\overline{u}(r)$ and only depends on $r = (x^2 + z^2)^{1/2}$, which increases from the pipe center to the wall [38]. A typical approach for this profile is given by,

$$\overline{u}(r) = \overline{U}_{\max}\left(1 - \frac{r}{D/2}\right)^{\frac{1}{n}}\,, \tag{19}$$

where n varies with the Reynolds number ($Re = \overline{U}_m D\rho_f/\mu_f$) and, for a smooth pipe is expressed implicitly by the relation [39],

$$n = 2\log\left(\frac{Re}{n} - 0.8\right)\,. \tag{20}$$

For a given flow rate (expressed by Re), the maximum time-averaged velocity $\overline{U}_{\max}$ is related to the mean velocity as in [39],

$$\frac{\overline{U}_m}{\overline{U}_{\max}} = \frac{2n^2}{(n+1)(2n+1)}\,, \tag{21}$$

therefore, with this analytical solution, it is possible to find, for a given Re, the value of n using Equation (20) and an iterative method. Then, using Equation (21), $\overline{U}_{\max}$ is obtained to be used in Equation (19) to provide the time-averaged velocity profile. Finally, this profile is used in Equation (17) to compute the profile factor, k.

Under disturbed flow conditions, Equation (19) does not accurately represent the velocity distribution along the acoustic path, highlighting the need for a more robust approach to calculate the profile factor. For this purpose, the velocity field can be integrated along the acoustic path in the complete format [19,25] for the case presented in Section 2.1:

$$\overline{U}_{\mathrm{UFM}} = \frac{1}{L_{\mathrm{AP}}}\left(\int_{L_{\mathrm{AP}}} u\,d\vec{L} + \tan\alpha\cos\theta\int_{L_{\mathrm{AP}}} v\,d\vec{L} + \tan\alpha\sin\theta\int_{L_{\mathrm{AP}}} w\,d\vec{L}\right)\,. \tag{22}$$

Obtaining the complete velocity field, in turn, is not a simple task. Two possible techniques are commonly considered. The first one involves measuring it using experimental methods. Even in laboratory conditions, these measurements are quite sophisticated; in industrial installations, they are impractical. The second option is to model the flow,

either using analytical approximations or numerical simulations (CFD). In this work, we demonstrate how CFD can be used for this purpose, increasing the accuracy of ultrasonic flow meters under non-conforming measuring conditions (disturbed flows).

3. Numerical Simulations Supporting Ultrasonic Flow Measurement

The development of robust commercial codes and the growing use of CFD in industrial applications position numerical simulation as a strong candidate for metrology applications. In recent years, CFD has been extensively utilized in this context. Although the phenomena related to ultrasonic flow measurement possess a multiphysics character, here, we emphasize what is strictly related to fluid dynamics. This section begins with a historical overview of the application of CFD, specifically focusing on ultrasonic flow measurement. It will then discuss the prominent ways in which CFD has been applied to assist ultrasonic flow measurement.

The seminal work by Holm et al. [40] brought significant attention to the application of CFD for calculating the profile factor under disturbed conditions, highlighting the potential of CFD to meet metrological requirements. Building on this foundation, Hilgenstock and Ernst [41] explored various pipe fittings to compare simulated and experimentally measured velocity profiles, assessing the differences between these profiles as a function of different acoustic path configurations and pipe setups. Increasing the complexity, Yeh and Mattingly [42] coupled the fluid simulation with an acoustic model for disturbed and undisturbed flow conditions. After those pioneers' works, several other studies used CFD for a wide range of analyses. CFD has been used to evaluate the effect of transducer protrusion and recess [43], to integrate the velocity and acoustic fields [44], and to promote general improvements for ultrasonic flow measurement and flow meter calibration [32], particularly, integrating CFD and artificial intelligence [45]. Beyond direct applications, fundamental advances are also highlighted. Important contributions aiming to improve the reliability of CFD results have been appearing in the last years, either by thorough investigations of the effect of simulation parameters [19,46] or by the quantification of simulation uncertainties [25,26]. Some of the recent developments are further discussed below. They deserve special attention mainly for delineating a refined and consistent way to use CFD as a tool for improving ultrasonic flow measurements.

3.1. Optimal Installation Configuration

Provided that the acoustic path is properly stabilized between the transducers, achieving the desired level of uncertainty relies heavily on the installation configuration, which is crucial for ensuring accurate measurements. Typically, transducers are strategically positioned along the pipeline to capture ultrasonic signals effectively. The orientation of the emission plane and the angles related to the streamwise direction and the transducers (θ and α, respectively, as illustrated in Figure 1) are critical for meeting accuracy requirements. The impact of installation location on measurement fidelity may vary considerably, influenced by factors such as the presence of elbows and other pipe fittings. CFD facilitates the virtual testing of distinct configurations, enabling an in-depth analysis of the installation effects. This methodology aids in identifying the optimal positioning, thereby minimizing measurement errors.

Simulations explore invasive [47] and noninvasive [33] ultrasonic transducer configurations, focusing on how installation affects measurement accuracy. Noninvasive installations are especially complex due to the need for high-precision acoustic transmission through multiple interfaces (e.g., transducer wedge, pipe wall, flowing fluid) and the geometric considerations inherent in complex pipelines. In this context, CFD can be applied to identify and mitigate these challenges, ensuring optimal placement and signal clarity [48].

The work by Martins et al. [19] seeks to identify optimal installation setups by analyzing the influence of disturbances (varying pipe fittings) on flow measurement. Simulations show that parameters like Reynolds number, inlet velocity profile, and transducer installation angle (θ) significantly affect flow readings close to disturbances. To reduce such errors in UFM readings, placing the meters at a specific distance downstream (typically around 30 pipe diameters from disturbances) and choosing θ strategically are crucial aspects to minimize the effects of upstream flow irregularities. Aligned with this study, Piechota et al. [49,50] discuss various setups, particularly configurations after a hydraulic elbow, and recommend specific angles and distances for optimal measurement. The study explores the configuration of a transit-time ultrasonic flow meter at varying distances from the elbow, suggesting that for accurate readings, the placement of transducers aligned with the flow direction at distances beyond ten diameters (10D) from the elbow yielded results close to pre-obstacle velocities. Transducer installation angle adjustments are necessary for measurements closer to the elbow due to significant velocity discrepancies influenced by turbulence.

The study of [51] investigates the effects of various path configurations and installation angles on measurement accuracy in n-path multi-path ultrasonic phased array flow meters (see [52] for more details about such flow meter). Nouri and Sakhavi [51] identify optimal path arrangements for three- and five-path configurations, specifically for flow scenarios downstream of single and double bends. For instance, a configuration of [$\pm$70°, $\pm$35°, 0°] achieves minimal error downstream of a single bend. In contrast, [$\pm$65°, $\pm$25°, 0°] is optimal downstream of a double bend. These configurations help reduce errors caused by non-ideal, asymmetric flow profiles common in bent pipeline installations.

3.2. Design Optimization

Research on design optimization pushed by new CFD-coupled tools brings, without doubt, new insights to design flow circuits and parts optimized to reduce losses in flow measurements [19]. In a direct, more simple form, design optimization could involve selecting the model that best corresponds to the typical flow conditions expected in the specific application, enabling accurate, consistent measurements, such as that proposed by [53]. However, more robust and sophisticated tools have recently been made available, although under commercial licenses [54].

Design optimization topic, mainly through geometry improvement, is a significant focus within the works of Rincón et al. [13,55,56], which centers on enhancing ultrasonic flow meters using CFD and advanced optimization techniques. The authors employ CFD and enhanced turbulence modeling to refine the shape and structure of flow meter components. The design optimization process in [55,56] starts with parameterizing the geometry of the flow meter. Parameters include key design variables such as stand and transducer locations and shapes. Initial simulations establish baseline models, which are validated through experimental data. Various optimization techniques were employed to predict the flow behavior and improve geometry, including Bayesian and surrogate-based optimization methods. A unique feature of this optimization approach is using surrogate models, which approximate the CFD results with minimal computation. Through techniques like multi-objective Pareto optimization, the design process balances conflicting objectives (e.g., reducing pressure drop while maintaining measurement accuracy). This aspect is crucial, as it allows designers to achieve improved flow characteristics in the meter without compromising on critical functional requirements. The workflow of this process extracted from [56] is presented in Figure 6.

After the initial optimization, further refinements are applied using adjoint-based shape optimization. This technique allows detailed and continuous geometry modification

by morphing the surfaces of components. As a result, the optimized shapes can achieve higher performance gains than achievable through parameter-based optimizations alone.

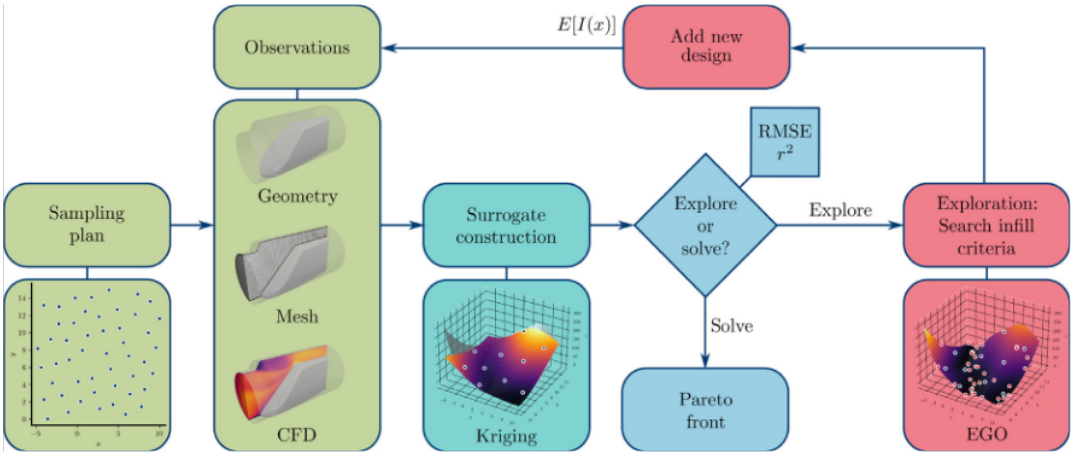

Figure 6. Workflow from [56] for optimizing ultrasonic flow meter designs. This diagram illustrates the process of optimizing ultrasonic flow meter designs using CFD and surrogate modeling. The workflow begins with creating a sampling plan, followed by geometry and mesh generation. CFD simulations are then executed to gather observations. A surrogate model is constructed using Kriging interpolation to approximate the design space. At a critical decision point, the process determines whether to explore the design space further or solve for optimal solutions. Exploration utilizes the Expected Improvement (EGO) criterion to refine the surrogate model, while solving results in the generation of the Pareto front for multi-objective optimization. Model accuracy is assessed using metrics such as Root Mean Square Error (RMSE) and r^2. New designs are iteratively added to the process to enhance optimization.

3.3. CFD-Assisted Ultrasonic Flow Measurement

One of the main intentions of using CFD in ultrasonic flow measurements is to estimate profile factor correlations for non-conforming installations. In view of the flow measurement uncertainty requirements, any disturbance in the velocity profile in the measuring section implies a potential need for correction, as explained in Section 2.4. For that purpose, well-executed CFD can provide reliable estimates of the velocity field of a given installation. With that in hand, it is possible to place virtual flow meters with desired position along a straight pipe length, installation angle, in single- or multi-path arrangements, etc. [19,24,26]. Furthermore, one can integrate the velocity profile and calculate the virtual profile factor associated with it. In this connection, the profile factor of a virtual flow meter can be compared with a theoretical one, which, in turn, is obtained by an empirical correlation or by a theoretical velocity profile at a given Reynolds number, and the relative difference between them is an estimate of the deviation of the flow rate measurement.

The possibility of virtual profile factors allows for their potential use in real ultrasonic flow measurement installations. The most intuitive idea would be to enter simulated profile factor correlations in an ultrasonic flow meter under non-conforming conditions. With a significant amount of CFD results, a *dynamic* profile factor correlation could be implemented for disturbed flow conditions. Another approach is to use the results of virtual flow meters as a design tool, indicating more favorable configurations for position and angle of installation. The restriction for this is mainly centered on the reliability of the results obtained by the numerical simulation itself. In industrial applications, the quantification of uncertainties associated with numerical simulations is not customary. Also, disturbed internal flow is somewhat challenging for RANS turbulence models [27]. Achieving high levels of fidelity in simulations is crucial for evolving to this scenario in which CFD

can be used as a tool not only to evaluate and assist but to actually improve ultrasonic flow measurement.

3.4. A Pragmatical Framework to Use CFD as an Analysis Tool

To summarize the use of CFD for the purpose discussed in Section 3.3, this section presents a pragmatical framework, based on previous works, to provide a solid path to use CFD as a virtual flow meter. It aims to enable the use of CFD as a reliable analysis tool to evaluate the flow measurement—more particularly, to calculate the profile factor—under disturbed flow conditions.

The procedure to obtain the so-called disturbed profile factor is presented in Figure 7.

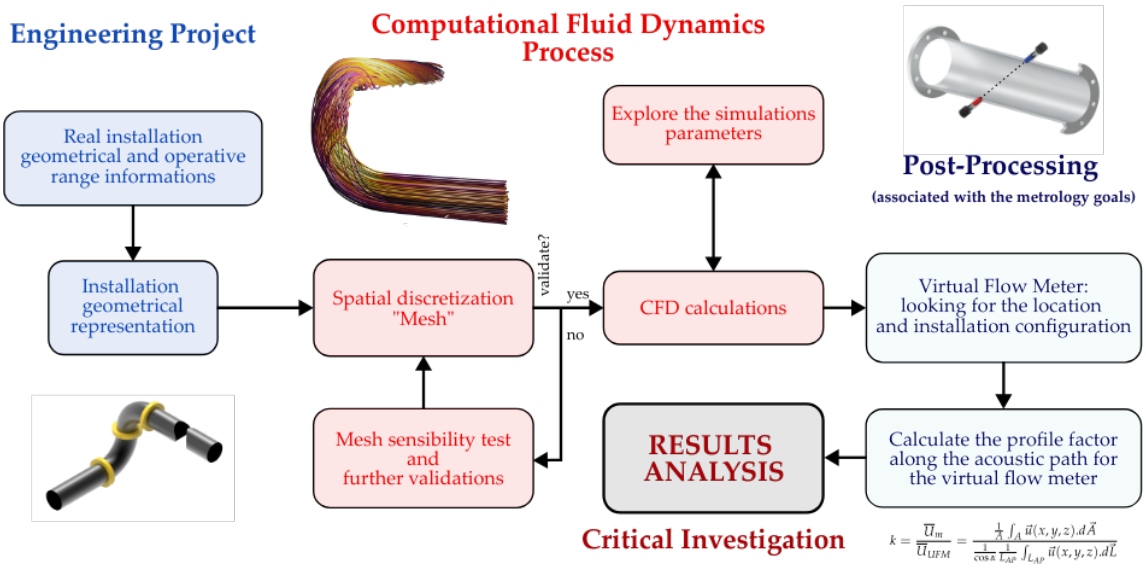

Figure 7. Framework to use computational fluid dynamics to analyze the profile factor under disturbed flow conditions.

The eminent step is to obtain information about the operation condition at the installation where the meter is/will be installed. The goal is to obtain the most representative geometry that contains the pipe fitting (e.g., curves, tees, etc.) and also the possible elements that could disturb the flow and affect the measurement (e.g., valves, downstream sensors, etc.). In this step (*Engineering Project* in Figure 7), it is necessary to find the most important elements in the pipeline but also to make the simplifications to obtain a feasible geometry for the simulations. Also, the knowledge of the usual flow rate condition on this installation is essential for the simulation to be dynamically similar to the real condition. It is important to highlight that, at this point, the choice of the domain of interest is intrinsically connected with the boundary conditions for the numerical simulations, which are as important as difficult to determine. Usually, the flow upstream from the measurement section contains—besides the pipe fitting itself—a vessel or a turbomachine. Any cross-section is challenging as an inlet condition for CFD calculations.

Once the geometry is defined and accurately reflects the real conditions, the CFD analysis can proceed according to the steps outlined in Figure 7. A critical aspect of this process is to evaluate how the choice of spatial discretization influences the results. While this evaluation is essential, there is currently no consensus in the literature on a systematic approach to achieving it, and a detailed discussion is beyond the scope of this paper. The goal is to obtain results that are independent of spatial discretization. This can often be achieved by progressively refining the mesh throughout the domain. This also depends on the available computational resources and the required or acceptable levels

of uncertainty for the model. When experimental results are available, comparing the numerical findings with those experimental data is preferable to validate the outcomes. Once spatial discretization independence is established (when applicable), it is time to assess the influence of various numerical simulation parameters, such as turbulence models, inlet conditions, etc., as previously discussed by the authors in [25]. This step, together with an appropriate uncertainty quantification technique [26], can provide the velocity field in the domain within a confidence interval.

Using the velocity field and leveraging numerical simulations, one can thoroughly examine various meter configurations through the virtual flow meter approach. In this context, each acoustic path is virtually represented as a straight line during the post-processing stage. Along these lines, data regarding the velocity field can be extracted, allowing for the calculation of the profile factor (refer to Equations (17) and (22)). The resulting data, for instance, could be assessed to meet the objectives outlined in Section 3.1 and Section 3.3.

Other important aspects related to numerical simulations—and hard to deal with—regard the fact that they depend on detailed knowledge of the industrial process involved in the flow measurement. They include the following, among others: How to define reliable boundary conditions at the inlet and outlet of a model domain in the presence of an upstream pressure vessel or a pump? How to estimate the turbulence intensity? This is a challenge for those conducting analysis by CFD and for the industries as well. For the former, to be conscious of these (and other) issues and to know strategies to overcome them. For the latter, to try to provide instrumentation and data enough and necessary for simulations.

4. Perspectives

With growing applications across diverse industries, ultrasonic flow measurement technology continues to evolve to meet stringent accuracy, efficiency, and operational flexibility requirements. Numerical simulations play a crucial role in achieving these advancements by offering a powerful platform for inferring flow characteristics and optimizing UFM installations under various operational conditions. However, as the complexity of UFM applications increases, further enhancements in CFD approaches and integration with new technologies are necessary to meet specific measurement challenges or requirements.

This section explores key perspectives in CFD for enhancing UFM applications, including the potential of high-resolution simulations like LES and DNS, the coupling of fluid dynamics with acoustic modeling, and the integration of artificial intelligence (AI) and machine learning (ML) techniques. Additionally, we discuss the importance of simulation uncertainty quantification and sensitivity analysis on simulation parameters to ensure reliable, high-accuracy measurements. These advancements will enable CFD to address a broader range of UFM challenges, providing a foundation for further ultrasonic flow measurement technology improvements.

4.1. Hybrid-RANS-LES, LES, and DNS

Dealing with the modeling of turbulent flows via CFD is a classic challenge. The search for more accurate results with a reasonable computational cost still defies researchers worldwide. The history of UFMs mainly points to the RANS approach as a tool to simulate pipe flows. In this section, we discuss the actual essay on other possibilities, their applicability, and we infer how further advances can improve UFM simulations.

Firstly, in a general view, we recall that RANS, LES, and DNS are approaches to turbulence, not models. In fact, DNS reflects the absence of turbulence models, while the LES and RANS perspectives are an open field for turbulence models, which is a broad subject and is beyond the scope of this communication. Even so, it is important to mention

that each of the RANS and LES models has their pros and cons, mainly for being conceived to treat specific problems. Therefore, finding a turbulence model that performs well for any physical phenomenon is a huge challenge. Usually, it depends on several flow characteristics. For more details on the different RANS and LES models, their formulation, applicability, advantages, and disadvantages, the reader is referred to [57–59]. LES and DNS are advanced CFD methods that provide highly detailed insights into turbulent flows, which are crucial for refining UFM accuracy in non-ideal flow conditions. LES filters out smaller eddies to focus on capturing the larger, energy-carrying flow structures, effectively maintaining accuracy without fully resolving all turbulence scales. In contrast, DNS resolves every turbulent eddy directly, offering the most detailed view of flow dynamics, but at a significantly higher computational cost.

At this point, it is important to distinguish fundamental from technological contributions. On the one hand, although DNS and LES are still computationally costly, their results are basal for helping the advancement of knowledge on the physics underlying the flow phenomena [27,60,61], developing more accurate turbulence models, and precisely in the context of UFM, accessing more accurate velocity fields around measuring sections—either for straight [62] or bent pipes—which enable estimating more accurate profile factors and, consequently, flow rates.

On the other hand, it is necessary to respond to industry demands with compatible deadlines and expectations. For that, RANS-based models still prevail, even though with restrictions. Particularly for UFMs, one of the main interests is to deal with non-conforming flow conditions, which involve adverse pressure gradients and highly anisotropic Reynolds stress states [63], a known obstacle for the majority of turbulence models. Still referring to UFMs, recent tests have already shown that uncertainties related to the profile factor can be reduced when hybrid RANS-LES approaches are used instead of regular RANS models, albeit at a higher cost [26]. Interestingly, RANS models are still suitable if the evaluated measuring sections are located up to 10 D downstream from a bend [46]. RANS models tend to overestimate the swirl effect for greater distances, which indicates that hybrid RANS-LES seems to be preferred in this context [46].

A clear path for allowing CFD to be a more useful tool for improving ultrasonic flow measurements is providing more accurate data on flows under disturbed conditions. Extending approaches similar to the one of Liu et al. [62] to disturbed profiles is pivotal for advancing flow measurement simulations. Therefore, we challenge the community to perform, communicate, and make available more accurate data of disturbed flow, either from LES or DNS (or even experiments!).

4.2. Multiphysics Approaches

Due to its working principle and operational conditions, ultrasonic flow measurement installations are typically multiphysical. One can list, at least, acoustics, fluid dynamics, signal processing, and thermodynamics. Furthermore, the problem is intrinsically dynamic. Thus, a fair simulation would account for every underlying physics in a time-dependent framework. Needless to say, this is currently impractical.

Among many simplifications, the acoustic path is considered a straight line virtually connecting a pair of transducers. As discussed in Section 2, this is somewhat reasonable for flows at low (below 0.1) Mach number (Mach number in this context is the ratio between the mean cross-section velocity and the speed of sound in the fluid). Above that, the sound drift phenomenon becomes relevant, and although the steered angle is dependent on the average mean flow velocity only, the propagating time depends on the velocity profile [64]. Thus, when important and increasing restrictions are considered, it is fundamental to be aware of the deviations experienced by the ultrasonic pulse and how these deviations

affect the reading of ultrasonic flow meters. This is even more important when the flow undergoes disturbances because the acoustic ray deviations are dependent on velocity and speed of sound gradients [42].

When modeling the propagation of sound in moving inhomogeneous media, the so-called ray theory is often used [65]. Recent advances in this type of coupled hydrodynamics–acoustics simulation are still limited to somewhat simplified velocity profiles [44,66,67]. Even though relevant advances have been reported recently, they are mainly related to the estimation of the profile factor [44] and the error due to the non-uniformity of the velocity profile [67]. However, more investigation is needed to evaluate the effect of elasticity at the pipe walls [68] and the sound drift under realistic disturbed velocity profiles.

Other approximations—mostly thermochemical—are very common, mainly to facilitate or even allow engineering responses. To list a few, one could still use CFD and consider the effect of fluid temperature [16,69–71] or pressure, complex fluid composition (mainly in gases) that can cause attenuation of the ultrasonic signal power [72], the presence of water in gases [73,74], and eventual phase changes during the flow.

It is worth noting that these multiphysics phenomena are often related to each other. Therefore, it is still very challenging to perform a robust multiphysics approach using CFD to simulate ultrasonic flow measurement installations. However, we are getting closer to carrying out simulations that incorporate more physics into the problem. This will undoubtedly bring more knowledge and challenges.

4.3. AI and ML Integration for UFM Calibration and Prediction

The integration of AI and ML techniques into UFM has significant potential for automating calibration, optimizing profile factors, and improving predictive accuracy. Recent research demonstrates that AI methods, including principal component analysis (PCA), symbolic regression, random forests, and artificial neural networks (ANNs), can substantially enhance UFM performance by predicting and compensating for flow profile variations, reducing calibration frequency, and refining error prediction models. Notwithstanding, we call the reader's attention to the fact that using AI and ML with simulation results requires reliable and accurate data to feed the algorithms, which are not trivial to obtain.

In a recent study [75], PCA is applied to model asymmetric velocity profiles that frequently disrupt UFM accuracy in complex flow conditions. The incorporation of PCA enables the UFM to dynamically adjust profile factors and optimize measurements across various flow regimes, enhancing the meter's accuracy even in challenging installations. Another promising approach that supports UFM advancements is symbolic regression coupled with active learning [76]. This model iteratively refines models based on selected CFD data points, reducing computational costs while providing interpretable, symbolic equations for flow behavior. This process is especially valuable for UFMs in non-standard installations where symbolic equations can replace complex simulations, enabling real-time flow predictions that are adaptable to various pipe configurations.

Other remarkable recent advances also inspire future CFD-AI integrated methods to enhance UFM performances. For instance, an experimentally-based multi-layer perceptron neural network has already been used to improve the calibration of UFMs [45]. Also, random forests and ANNs allow a real-time error prediction in UFM applications by analyzing key flow characteristics, such as the signal-to-noise ratio, flow velocity, and profile factors, to predict deviations from reference measurements [77]. Additionally, the integration of mechanistic and data learning in a loss function design has shown promising results in predicting accurate velocity field and flow rates [78].

The integration of AI and ML methods into UFM systems supports a data-driven approach to calibration, which is especially beneficial for UFMs in fluctuating operational environments. These methods provide the following advantages:

- Reduced Calibration Frequency: By automating flow pattern adjustments through PCA and real-time error predictions via random forests and ANNs, UFMs can maintain accuracy over extended periods with minimal recalibration.
- Enhanced Predictive Accuracy in Complex Flows: Symbolic regression-based models offer simplified yet accurate equations derived from CFD data, enabling UFMs to predict flow rates in non-standard and asymmetric installations.
- Improved Operational Insights: Feature importance analysis in RF models can identify critical parameters affecting measurement accuracy, guiding targeted improvements in UFM design and calibration practices.

In summary, the integration of AI and ML techniques into UFMs can transform flow measurement, enabling these meters to adapt dynamically to various industrial conditions. This shift represents a substantial step forward in UFM technology, with AI-driven capabilities for self-adjustment and predictive error correction supporting greater reliability and precision across diverse applications. Nevertheless, using CFD as a tool to provide information for AI-driven models requires reliable simulations, which reinforces the need for more accurate simulations together with rigorous uncertainty quantification and statistical approaches.

4.4. Progresses in the CFD Approach

The continual improvement of CFD methods is vital for enhancing the accuracy and reliability of UFM. In recent years, significant advances have been made in two critical areas: simulation uncertainty quantification and the evaluation of the effect of simulation parameters.

Simulation uncertainty quantification ensures the reliability of CFD-based virtual measurements. Rigorous uncertainty frameworks allow CFD to deliver results with confidence levels comparable to physical measurements, such as a 95.45% confidence interval [26]. The adoption of uncertainty quantification frameworks is essential to bridge the gap between experimental and virtual measurements. By integrating rigorous verification and validation processes, CFD simulations can provide traceable, high-confidence results that meet industrial metrological standards. An example of how uncertainty quantification of simulated results can be reported is shown in Figure 8.

Moreover, improving the accuracy of CFD simulations not only supports direct UFM applications but also serves as a foundation for data-driven methods. High-fidelity CFD data can be used as input for AI and ML models, enabling advanced calibration and real-time prediction of flow behavior in dynamic environments. This synergy between CFD and AI/ML presents a promising avenue for reducing reliance on experimental calibration and further automating UFM systems.

The accuracy of CFD simulations in the context of UFM strongly depends on the choice of simulation parameters. Choices related to turbulence models, boundary conditions, mesh resolution, and numerical schemes significantly affect the calculated flow fields and, consequently, the profile factors used in ultrasonic flow measurement [25,46]. These findings underline the importance of systematically verifying the influence of key simulation parameters to ensure reliable CFD predictions.

A robust verification process not only improves the accuracy of CFD results but also builds confidence in their use for practical applications, such as UFM calibration and design optimization. As regulatory bodies begin to recognize CFD as a valid tool for flow measurement in non-standard installations, it is imperative to standardize sensitivity anal-

ysis practices across the field. This systematic approach will enable the broader adoption of CFD in industrial metrology, supporting more accurate and reliable ultrasonic flow measurement installations.

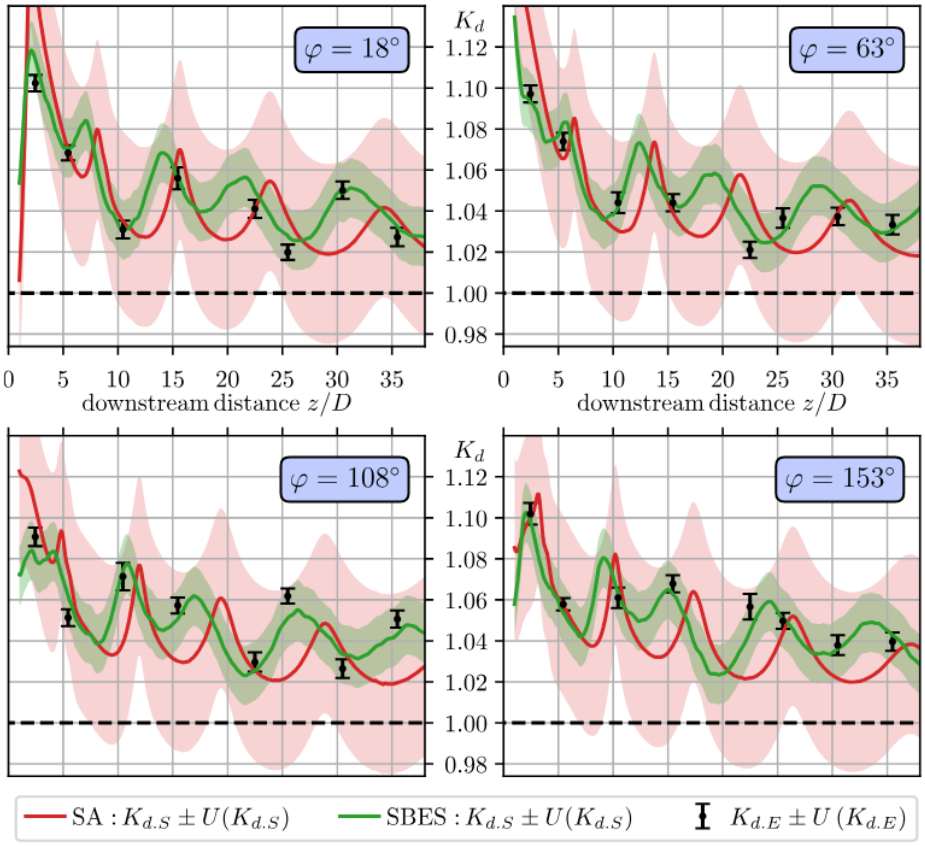

Figure 8. Figure from [26] showing the simulation-based profile factors (K_d) with their respective uncertainty. Their analysis assesses four different configurations varying the installation angle (φ = 18°, 63°, 108°, and 153°). The red color refers to the Spalart–Allmaras (SA) model, the green color represents the stress-blended eddy simulation (SBES) model, and the symbols with bars are related to experimental measurements.

5. Conclusions

Since the 1990s, CFD has been used as a tool to help understand challenging situations related to ultrasonic flow measurement. The main issues are as follows: (i) the interaction between acoustic rays and fluid flow and (ii) the effect of disturbed flows on the measurement of the flow rate. Whether using restrictive assumptions or not, the actual challenges of ultrasonic flow measurement that can use CFD as a tool depend on simulations of ever-increasing fidelity. Thus, it is crucial that researchers synergistically build a path to allow these improvements. In this sense, several branches of research appear: the improvement of turbulence modeling for disturbed pipe flows, publication and availability of experimental results of disturbed velocity fields and flow meter performances for validation, analysis of effects caused by simulation parameters such as inlet conditions, and evaluation of several simulations integrated with robust statistical analysis to identify variations and quantify simulation uncertainties.

When these research areas undergo substantial progress, maybe we will be able to generate more reliable results from CFD and focus on advancing, for instance, the integration of fluid dynamics and acoustic rays in even more realistic frameworks, the simulation of strong dynamic effects on ultrasonic flow measurements (such as high turn-down ra-

tios during operations), and the usage of profile factor correlations obtained by CFD in real industrial UFMs, which requires not only the credibility of CFD results but also legal recognition for metrological purposes. These advances would make ultrasonic flow measurement much better and smoother in any industrial context.

Judging by the present scenario, it is evident that we are already heading towards great advances. It is difficult to predict how long it would take until we reach a comfortable and feasible level of confidence in the results obtained by CFD to actually push ultrasonic flow measurements significantly forward. For those interested in this subject, it is essential to keep working consistently towards more robust turbulence modeling, communicating CFD results with uncertainty quantification and proper statistics, and, as long as possible, integrating complete physics and artificial intelligence techniques.

Author Contributions: Conceptualization, G.S.d.A., R.S.M., M.F.M. and R.R.; methodology, G.S.d.A. and R.S.M.; formal analysis, G.S.d.A. and R.S.M.; investigation, G.S.d.A., R.S.M. and M.F.M.; resources, M.F.M. and R.R.; writing—original draft preparation, G.S.d.A. and R.S.M.; writing—review and editing, G.S.d.A., R.S.M., M.F.M. and R.R.; project administration, R.R.; funding acquisition, R.R. All authors have read and agreed to the published version of the manuscript.

Funding: This research was funded by Petrobras (Brazil) grant number 2018/00194-3 and 2024/00300-9.

Data Availability Statement: Data sharing is not applicable.

Conflicts of Interest: The authors declare no conflicts of interest.

References

1. Mylvaganam, K. High-rangeability ultrasonic gas flowmeter for monitoring flare gas. *IEEE Trans. Ultrason. Ferroelectr. Freq. Control* **1989**, *36*, 144–149. [CrossRef] [PubMed]
2. Emam, E.A. Gas Flaring in industry: An overview. *Pet. Coal* **2015**, *57*, 532–555.
3. Matson, J.; Sui, L.; Nguyen, T.H. Ultrasonic Flare Gas Flow Meter Techniques for Extremes of High and Low Velocity Measurement and Experience with High CO_2 Concentration. In Proceedings of the 28th International North Sea Flow Measurement Workshop, St. Andrews, UK, 26–29 October 2010.
4. Tan, C.; Murai, Y.; Liu, W.; Tasaka, Y.; Dong, F.; Takeda, Y. Ultrasonic Doppler Technique for Application to Multiphase Flows: A Review. *Int. J. Multiph. Flow* **2021**, *144*, 103811. [CrossRef]
5. The World Bank. Gas Flaring Explained. Available online: https://www.worldbank.org/en/programs/gasflaringreduction/gas-flaring-explained (accessed on 9 July 2023).
6. Mansoor, R.; Tahir, M. Recent developments in natural gas flaring reduction and reformation to energy-efficient fuels: A review. *Energy Fuels* **2021**, *35*, 3675–3714. [CrossRef]
7. Rodrigues, A. Decreasing natural gas flaring in Brazilian oil and gas industry. *Resour. Policy* **2022**, *77*, 102776. [CrossRef]
8. Motte, J.; Alvarenga, R.A.; Thybaut, J.W.; Dewulf, J. Quantification of the global and regional impacts of gas flaring on human health via spatial differentiation. *Environ. Pollut.* **2021**, *291*, 118213. [CrossRef]
9. The World Bank. Global Gas Flaring Reduction Partnership (GGFR). 2023. Available online: https://www.worldbank.org/en/programs/gasflaringreduction (accessed on 11 March 2023).
10. Tobin, J.; Shambaugh, P.; Mastrangelo, E. *Natural Gas Processing: The Crucial Link Between Natural Gas Production and Its Transportation to Market*; Energy Information Administration, Office of Oil and Gas: Washington, DC, USA, 2006.
11. ANP (Agência Nacional de Petróleo, Gás e Biocombustível). ANP Resolution Number 806. 20 January 2020. Available online: https://atosoficiais.com.br/anp/resolucao-n-806-2020-regulamenta-os-procedimentos-para-controle-de-queima-e-perda-de-petroleo-e-de-gas-natural?origin=instituicao&q=806 (accessed on 21 November 2023).
12. Davoudi, M.; Rahimpour, M.; Jokar, S.; Nikbakht, F.; Abbasfard, H. The major sources of gas flaring and air contamination in the natural gas processing plants: A case study. *J. Nat. Gas Sci. Eng.* **2013**, *13*, 7–19. [CrossRef]
13. Rincón, M.; Caspersen, A.; Ingwersen, N.; Reclari, M.; Abkar, M. Flow investigation of two-stand ultrasonic flow meters in a wide dynamic range by numerical and experimental methods. *Flow Meas. Instrum.* **2024**, *96*, 102543. [CrossRef]
14. Chen, D.; Cao, H.; Cui, B. Study on flow field and measurement characteristics of a small-bore ultrasonic gas flow meter. *Meas. Control* **2021**, *54*, 554–564. [CrossRef]
15. Jung, J.C.; Seong, P.H. Estimation of the flow profile correction factor of a transit-time ultrasonic flow meter for the feedwater flow measurement in a nuclear power plant. *IEEE Trans. Nucl. Sci.* **2005**, *52*, 714–718. [CrossRef]

16. Tawackolian, K.; Büker, O.; Hogendoorn, J.; Lederer, T. Calibration of an ultrasonic flow meter for hot water. *Flow Meas. Instrum.* **2013**, *30*, 166–173. [CrossRef]
17. AGA. *Measurement of Gas by Multipath Ultrasonic Meters*; Report No. 9; American Gas Association: Washington, DC, USA, 2007.
18. Lynnworth, L.; Liu, Y. Ultrasonic flowmeters: Half-century progress report, 1955–2005. *Ultrasonics* **2006**, *44*, e1371–e1378. [CrossRef] [PubMed]
19. Martins, R.S.; Andrade, J.R.; Ramos, R. On the effect of the mounting angle on single-path transit-time ultrasonic flow measurement of flare gas: A numerical analysis. *J. Braz. Soc. Mech. Sci. Eng.* **2020**, *42*, 13. [CrossRef]
20. Westerweel, J.; Elsinga, G.; Adrian, R. Particle Image Velocimetry for Complex and Turbulent Flows. *Annu. Rev. Fluid Mech.* **2013**, *45*, 409–436. [CrossRef]
21. Alaeddin, M.A.; Hashemabadi, S.H.; Mousavi, S.F. Numerical study on the effect of circumferential position of ultrasonic transducers on ultrasonic cross-correlation flowmeter performance under asymmetric air flow profile. *Ultrasonics* **2021**, *115*, 106479. [CrossRef]
22. Hallanger, A.; Saetre, C.; Frøysa, K.E. Flow profile effects due to pipe geometry in an export gas metering station—Analysis by CFD simulations. *Flow Meas. Instrum.* **2018**, *61*, 56–65. [CrossRef]
23. Weissenbrunner, A.; Fiebach, A.; Schmelter, S.; Bär, M.; Thamsen, P.; Lederer, T. Simulation-based determination of systematic errors of flow meters due to uncertain inflow conditions. *Flow Meas. Instrum.* **2016**, *52*, 25–39. [CrossRef]
24. Geršl, J.; Knotek, S.; Belligoli, Z.; Dwight, R.; Robinson, R.; Coleman, M. Flow rate measurement in stacks with cyclonic flow—Error estimations using CFD modelling. *Measurement* **2018**, *129*, 167–183. [CrossRef]
25. Martins, R.S.; de Aquino, G.S.; Martins, M.F.; Ramos, R. Sensitivity analysis for numerical simulations of disturbed flows aiming ultrasonic flow measurement. *Measurement* **2021**, *185*, 110015. [CrossRef]
26. Straka, M.; Weissenbrunner, A.; Koglin, C.; Höhne, C.; Schmelter, S. Simulation Uncertainty for a Virtual Ultrasonic Flow Meter. *Metrology* **2022**, *2*, 335–359. [CrossRef]
27. Kalpakli Vester, A.; Örlü, R.; Alfredsson, P.H. Turbulent Flows in Curved Pipes: Recent Advances in Experiments and Simulations. *Appl. Mech. Rev.* **2016**, *68*, 050802. [CrossRef]
28. Miller, R. *Flow Measurement Engineering Handbook*; Chemical Engineering Books; McGraw-Hill Education: New York, NY, USA, 1996.
29. Carlander, C.; Delsing, J. Installation effects on an ultrasonic flow meter with implications for self diagnostics. *Flow Meas. Instrum.* **2000**, *11*, 109–122. [CrossRef]
30. Ren, R.; Wang, H.; Sun, X.; Quan, H. Design and Implementation of an Ultrasonic Flowmeter Based on the Cross-Correlation Method. *Sensors* **2022**, *22*, 7470. [CrossRef] [PubMed]
31. Kuhnicke, E. The limitations of Snell's law in the design of ultrasound transducers. In Proceedings of the 1999 IEEE Ultrasonics Symposium, Tahoe, NV, USA, 17–20 October 1999; Proceedings. International Symposium (Cat. No.99CH37027), Volume 2, pp. 1067–1070. [CrossRef]
32. Yeh, T.; Espina, P.; Osella, S. An Intelligent Ultrasonic Flow Meter for Improved Flow Measurement and Flow Calibration Facility. In Proceedings of the 18th IEEE Instrumentation and Measurement Technology Conference, IMTC 2001, Budapest, Hungary, 21–23 May 2001; Volume 3, pp. 1741–1746. [CrossRef]
33. Sanderson, M.; Yeung, H. Guidelines for the use of ultrasonic non–invasive metering techniques. *Flow Meas. Instrum.* **2002**, *13*, 125–142. [CrossRef]
34. Zhou, H.; Ji, T.; Wang, R.; Ge, X.; Tang, X.; Tang, S. Multipath ultrasonic gas flow-meter based on multiple reference waves. *Ultrasonics* **2018**, *82*, 145–152. [CrossRef]
35. Schröder, A.; Kupnik, M.; O'Leary, P.; Benes, E.; Gröschl, M. A Capacitance Ultrasonic Transducer With Micromachined Backplate for Fast Flow Measurements in Hot Pulsating Gases. *IEEE Sensors J.* **2006**, *6*, 898–905. [CrossRef]
36. Sakhavi, N.; Mohammad Nouri, N. Generalized velocity profile evaluation of multipath ultrasonic phased array flowmeter. *Measurement* **2022**, *187*, 110302. [CrossRef]
37. Moore, P.I.; Brown, G.J.; Stimpson, B.P. Ultrasonic transit-time flowmeters modelled with theoretical velocity profiles: Methodology. *Meas. Sci. Technol.* **2000**, *11*, 1802. [CrossRef]
38. Nikuradse, J. *Laws of Turbulent Flow in Smooth Pipes*; NASA TT F-10, 359; National Aeronautics and Space Administration: Washington, DC, USA, 1966; Translated from 'Gesetzmässigkeiten der turbulenten Strömung in glatten Rohren' Forsch. Arb. Ing.-Wes. No. 356 (1932).
39. Schlichting, H. *Boundary-Layer Theory*, 6th ed.; McGraw-Hill Series in Mechanical Engineering; McGraw-Hill: New York, NY, USA, 1968.
40. Holm, M.; Stang, J.; Delsing, J. Simulation of flow meter calibration factors for various installation effects. *Measurement* **1995**, *15*, 235–244. [CrossRef]
41. Hilgenstock, A.; Ernst, R. Analysis of installation effects by means of computational fluid dynamics—CFD vs experiments? *Flow Meas. Instrum.* **1996**, *7*, 161–171. [CrossRef]

42. Yeh, T.; Mattingly, G. Computer simulations of ultrasonic flow meter performance in ideal and non-ideal pipeflows. In Proceedings of the ASME Fluids Engineering Division Summer Meeting—FEDSM'97, Vancouver, BC, Canada, 22–26 June 1997; ASME: New York, NY, USA, 1997.
43. Zheng, D.; Zhang, P.; Xu, T. Study of acoustic transducer protrusion and recess effects on ultrasonic flowmeter measurement by numerical simulation. *Flow Meas. Instrum.* **2011**, *22*, 488–493. [CrossRef]
44. Mousavi, S.F.; Hashemabadi, S.H.; Jamali, J. Calculation of geometric flow profile correction factor for ultrasonic flow meter using semi-3D simulation technique. *Ultrasonics* **2020**, *106*, 106165. [CrossRef] [PubMed]
45. Yazdanshenasshad, B.; Safizadeh, M. Neural-network-based error reduction in calibrating utility ultrasonic flow meters. *Flow Meas. Instrum.* **2018**, *64*, 54–63. [CrossRef]
46. Ekat, A.K.; Weissenbrunner, A.; Straka, M.; Eichler, T.; Oberleithner, K. Hybrid LES/RANS Simulations of a 90° Pipe Bend Using Different CFD Solvers. *OpenFOAM® J.* **2023**, *3*, 49–65. [CrossRef]
47. Raišutis, R. Investigation of the flow velocity profile in a metering section of an invasive ultrasonic flowmeter. *Flow Meas. Instrum.* **2006**, *17*, 201–206. [CrossRef]
48. Luca, A.; Marchiano, R.; Chassaing, J.C. Numerical simulation of transit-time ultrasonic flowmeters by a direct approach. *IEEE Trans. Ultrason. Ferroelectr. Freq. Control* **2016**, *63*, 886–897. [CrossRef]
49. Piechota, P.; Synowiec, P.; Andruszkiewicz, A.; Wędrychowicz, W. Selection of the relevant turbulence model in a CFD simulation of a flow disturbed by hydraulic elbow—Comparative analysis of the simulation with measurements results obtained by the ultrasonic flowmeter. *J. Therm. Sci.* **2018**, *27*, 413–420. [CrossRef]
50. Piechota, P.; Synowiec, P.; Andruszkiewicz, A.; Wędrychowicz, W. Analysis of the accuracy of liquid flow measurements by the means of ultrasonic method in non-standard measurements conditions. In Proceedings of the Methods and Techniques of Signal Processing in Physical Measurements, Rzeszów-Arlamów, Poland, 17–20 September 2018; Springer: Cham, Switzerland, 2019; pp. 275–285.
51. Nouri, N.M.; Sakhavi, N. Numerical analysis of liquid flow measurement using multipath ultrasonic phased array flowmeter. *Ultrasonics* **2023**, *128*, 106859. [CrossRef]
52. Sakhavi, N.; Nouri, N.M. Performance of novel multipath ultrasonic phased array flowmeter using Gaussian quadrature integration. *Appl. Acoust.* **2022**, *199*, 109004. [CrossRef]
53. Willatzen, M. Flow acoustics modelling and implications for ultrasonic flow measurement based on the transit-time method. *Ultrasonics* **2004**, *41*, 805–810. [CrossRef]
54. Biancolini, M.E.; Capellini, K.; Costa, E.; Groth, C.; Celi, S. Fast interactive CFD evaluation of hemodynamics assisted by RBF mesh morphing and reduced order models: The case of aTAA modelling. *Int. J. Interact. Des. Manuf. (IJIDeM)* **2020**, *14*, 1227–1238. [CrossRef]
55. Rincón, M.J. Robust Optimisation of Ultrasonic Flow Meters by Computational Fluid Dynamics and Enhanced Turbulence Modelling. Ph.D. Thesis, Aarhus University, Aarhus, Denmark, 2023.
56. Rincón, M.J.; Reclari, M.; Yang, X.I.; Abkar, M. Validating the design optimisation of ultrasonic flow meters using computational fluid dynamics and surrogate modelling. *Int. J. Heat Fluid Flow* **2023**, *100*, 109112. [CrossRef]
57. Pope, S.B.; Pope, S.B. *Turbulent Flows*; Cambridge University Press: Cambridge, UK, 2000.
58. Versteeg, H.; Malalasekera, W. *An Introduction to Computational Fluid Dynamics—The Finite Volume Method*, 2nd ed.; Pearson Education Limited: Essex, UK, 2007.
59. Wilcox, D.C. *Turbulence Modeling for CFD*, 3rd ed.; DCW Industries: La Cañada, CA, USA, 2006.
60. Nygård, F.; Andersson, H.I. DNS of swirling turbulent pipe flow. *Int. J. Numer. Methods Fluids* **2010**, *64*, 945–972. [CrossRef]
61. Wang, Z.; Örlü, R.; Schlatter, P.; Chung, Y.M. Direct numerical simulation of a turbulent 90° bend pipe flow. *Int. J. Heat Fluid Flow* **2018**, *73*, 199–208. [CrossRef]
62. Liu, Z.g.; Du, G.s.; Shao, Z.f. The direct numerical simulation of pipe flow. *J. Hydrodyn.* **2013**, *25*, 125–130. [CrossRef]
63. de Aquino, G.S.; Martins, R.S.; Martins, M.F.; Ramos, R. Statistical considerations on RANS simulations of inhomogeneous pipe flows. *J. Braz. Soc. Mech. Sci. Eng.* **2025**, *47*, 60. [CrossRef]
64. Choudhary, K.P.; Arumuru, V.; Bhumkar, Y.G. Numerical simulation of beam drift effect in ultrasonic flow-meter. *Measurement* **2019**, *146*, 705–717. [CrossRef]
65. Koechner, H.; Melling, A. Numerical simulation of ultrasonic flowmeters. *Acustica* **2000**, *86*, 39–48.
66. Kupnik, M.; O'Leary, P.; Schroder, A.; Rungger, I. Numerical simulation of ultrasonic transit-time flowmeter performance in high temperature gas flows. In Proceedings of the IEEE Symposium on Ultrasonics 2003, Honolulu, HI, USA, 5–8 October 2003; Volume 2, pp. 1354–1359. [CrossRef]
67. Wang, Z.; Chen, Q.; Li, D.; Liu, S. Bias error in measurement of complex flow regime with ultrasonic flowmeter. *J. Phys. Conf. Ser.* **2022**, *2264*, 012031. [CrossRef]
68. Sun, Y.; Zheng, C.; Zhang, F.; Tan, X.; Chen, K.; Song, X.; Zhang, X.; Chen, Y. Theoretical study of elastic effect of a cylindrical pipe wall on ultrasonic flow measurement. *Measurement* **2023**, *219*, 113281. [CrossRef]

69. Bilaniuk, N.; Wong, G.S.K. Speed of sound in pure water as a function of temperature. *J. Acoust. Soc. Am.* **1993**, *93*, 1609–1612. [CrossRef]
70. Ge, L.; Deng, H.; Wang, Q.; Hu, Z.; Li, J. Study of the influence of temperature on the measurement accuracy of transit-time ultrasonic flowmeters. *Sens. Rev.* **2019**, *39*, 269–276. [CrossRef]
71. Kiefer, D.A.; Benkert, A.; Rupitsch, S.J. Transit Time of Lamb Wave-Based Ultrasonic Flow Meters and the Effect of Temperature. *IEEE Trans. Ultrason. Ferroelectr. Freq. Control* **2022**, *69*, 2975–2983. [CrossRef]
72. Franco, L.G. Methodologies to Mitigate Attenuating Effects in Flare Gas Flow Measurement by Ultrasonic Technology at Low Pressure and High Carbon Dioxide Concentration. Master's Dissertation, Universidade Federal do Espírito Santo, Vitória, ES, Brazil, 2020. Available online: https://sappg.ufes.br/tese_drupal//tese_14415_Dissertation%20FINAL%20LiGIA%20GAIGER%20FRANCO.pdf (accessed on 9 October 2022).
73. de Almeida, F.C.; de Oliveira, E.C.; Barbosa, C.R.H. Design of experiments to analyze the influence of water content and meter factor on the uncertainty of oil flow measurement with ultrasonic meters. *Flow Meas. Instrum.* **2019**, *70*, 101627. [CrossRef]
74. van Putten, D.S.; Dsouza, B.T. Wet gas over-reading correction for ultrasonic flow meters. *Exp. Fluids* **2019**, *60*, 45. [CrossRef]
75. Tran, N.; Wang, C.C. Enhancement of the accuracy of ultrasonic flowmeters by applying the PCA algorithm in predicting flow patterns. *Meas. Sci. Technol.* **2021**, *32*, 085901. [CrossRef]
76. Ansari, M.; Gandhi, H.A.; Foster, D.G.; White, A.D. Iterative symbolic regression for learning transport equations. *AIChE J.* **2022**, *68*, e17695. [CrossRef]
77. Li, M.; Li, Z.; Li, C. In-use measurement of ultrasonic flowmeter based on Machine learning. *Measurement* **2023**, *223*, 113721. [CrossRef]
78. Cai, H.; Liu, W.; Zhou, K.; Wang, X.; Lin, K.; Tang, X.Y. Physics Constrained High-Precision Data-Driven Modeling for Multi-Path Ultrasonic Flow Meter in Natural Gas Measurement. *Sensors* **2024**, *24*, 4521. [CrossRef]